The International Journal of Biochemistry & Cell Biology 45 (2013) 1223–1235

Contents lists available at SciVerse ScienceDirect

The International Journal of Biochemistry & Cell Biology

journal homepage: www.elsevier.com/locate/biocel

Calreticulin-dimerization induced by post-translational arginylation is critical for stress granules scaffolding

Marcos A. Carpio, María B. Decca, Cecilia Lopez Sambrooks, Edith S. Durand, Guillermo G. Montich, Marta E. Hallak*

Centro de Investigaciones en Química Biológica de Córdoba, CIQUIBIC, CONICET-Departamento de Química Biológica, Facultad de Ciencias Químicas, Universidad Nacional de Córdoba, Haya de la Torre y Medina Allende X5000HUA, Córdoba, Argentina

ARTICLE INFO

Article history:
Received 10 August 2012
Received in revised form 12 March 2013
Accepted 26 March 2013
Available online xxx

Keywords:
Calreticulin
Arginylation
Stress granules
Calcium
Dimerization

ABSTRACT

Protein arginylation mediated by arginyl-tRNA protein transferase is a post-translational modification that occurs widely in biology, it has been shown to regulate protein and properties and functions. Post-translational arginylation is critical for embryogenesis, cardiovascular development and angiogenesis but the molecular effects of proteins arginylated *in vivo* are largely unknown. In the present study, we demonstrate that arginylation reduces CRT (calreticulin) thermostability and induces a greater degree of dimerization and oligomerization. R-CRT (arginylated calreticulin) forms disulfide-bridged dimers that are increased in low Ca^{2+} conditions at physiological temperatures, a similar condition to the cellular environment that it required for arginylation of CRT. Moreover, R-CRT self-oligomerizes through non-covalent interactions that are enhanced at temperatures above 40 °C, condition that mimics the heat shock treatment where R-CRT is the only isoespecies of CRT that associates in cells to SGs (stress granules). We show that in cells lacking CRT the scaffolding of larger SGs is impaired; the transfection with CRT (hence R-CRT expression) restores SGs assembly whereas the transfection with CRT mutated in Cys146 does not. Thus, R-CRT disulfide-bridged dimers (through Cys146) are essential for the scaffolding of larger SGs under heat shock, although these dimers are not required for R-CRT association to SGs. The alteration in SGs assembly is critical for the normal cellular recover of cells after heat induced stress.

We conclude that R-CRT is emerging as a novel protein that has an impact on the regulation of SGs scaffolding and cell survival.

1. Introduction

Post-translational modifications (PTMs) of proteins perform crucial roles in regulating the biology of the cell because they can potentially change protein's physical or chemical properties, activity, localization or stability, controlling protein function, fate and cell signaling (Farley and Link, 2009). One of these PTMs is the incorporation of arginine into the N-terminus or into a glutamic residue at internal sites of the amino acid chain of proteins (Kaji et al., 1963; Barra et al., 1973; Wong et al., 2007; Rai et al., 2008), a reaction catalyzed by the arginyl-tRNA protein transferase (ATE1) (Soffer, 1971; Gonda et al., 1989; Bongiovanni et al., 1999). We have previously demonstrated the post-translational incorporation of arginine into calreticulin (CRT) *in vitro* and in cultured cells (Decca et al., 2007). CRT arginylation is required for its association to stress granules (SGs) which occurs under conditions that promote a decrease in intracellular Ca^{2+} levels, such as heat shock, thapsigargin (TG), TG-EGTA or arsenite treatment (Carpio et al., 2010). CRT is mainly localized in the lumen of the endoplasmic reticulum (ER) (Michalak et al., 2009) where it acts as a lectin and chaperone involved in the folding of new synthesized proteins (Zhang et al., 1997; Paquet et al., 2005; Labriola et al., 2011) as well as a modulator of Ca^{2+} homeostasis and signaling (Mailhot et al., 2000; Michalak et al., 2009; Bibi et al., 2011). Despite its ER retention KDEL signal, CRT can reach the cytoplasm and the plasma membrane by retrotranslocation (Afshar et al., 2005; Decca et al., 2007; Carpio et al., 2010; Lopez Sambrooks et al., 2012) where this protein is involved in multiple cell functions (Michalak et al., 2009; Gold et al., 2010; Wang et al., 2012). The Ca^{2+} binding to CRT plays a key role in the modulation of the different functions of this protein. CRT has two Ca^{2+} binding sites, a high-affinity, low capacity site located in the globular domain and a low-affinity, high-capacity site located in

Abbreviations: PTMs, post-translational modifications; ATE1, arginyl-tRNA protein transferase; CRT, calreticulin; R-CRT, arginylated CRT; SG, stress granule; TG, thapsigargin; ER, endoplasmic reticulum; DTT, dithiothreitol; TM, thermal denaturation temperature; CD, circular dichroism; Cys, cysteine; SH-Cys146, SH group of Cys146; mAb, monoclonal antibody; pAb, polyclonal antibody; TIA-1, T-cell intracytoplasmic antigen 1; WB, Western blot; MW, molecular weight.

* Corresponding author. Tel.: +54 351 5353855.
E-mail address: mhallak@fcq.unc.edu.ar (M.E. Hallak).

1357-2725/$ – see front matter © 2013 Elsevier Ltd. All rights reserved.
http://dx.doi.org/10.1016/j.biocel.2013.03.017

the C-terminal portion of the globular domain (Khanna et al., 1986; Baksh and Michalak, 1991; Wijeyesakere et al., 2011). The binding of Ca^{2+} at the high affinity binding site increases the thermal and chemical stability of CRT and enhances its resistance to protease digestion, suggesting a more rigid and well-packed tertiary structure of the protein (Corbett et al., 2000; Li et al., 2001). On the other hand, saturation of the low affinity Ca^{2+} binding site leads to a subtle reduction of the thermal stability of CRT, indicating further modulation of its conformation (Wijeyesakere et al., 2011).

CRT sequence only has three cysteine (Cys) residues situated in the amino acid positions 88, 120 and 146 (numbering is from residue 1 of mature CRT). Several studies demonstrate that an intramolecular disulfide bridge is formed between the Cys88 and Cys120, whereas the SH group of Cys146 (SH-Cys146) remains free. It has been demonstrated that disulfide-bridged homo-dimers of CRT are formed in non-reducing conditions, presumably after the exposure of the free SH-Cys146 (Jorgensen et al., 2003; Rizvi et al., 2004). In addition, the structural resolution of the globular domain of CRT shows that the intramolecular disulfide bridge is necessary for an efficient carbohydrate binding (Kozlov et al., 2010), CRT self-association as well as an increase in polypeptide binding/chaperone activity are promotes by Ca^{2+} depletion (Corbett et al., 2000; Rizvi et al., 2004; Wijeyesakere et al., 2011). Other conditions that favor partial CRT unfolding, such as high temperature, low pH (5–6) and chemical denaturant, also promote non-covalent CRT self-oligomerization (Jorgensen et al., 2003). CRT oligomerization *in vivo* had been related to an increase in chaperone activity upon heat shock or TG treatment (Rizvi et al., 2004). Interestingly, both of these treatments also improve *in vivo* CRT arginylation (Decca et al., 2007; Carpio et al., 2010). Thus, it is possible that both processes are achieved concomitantly within the cytoplasm. Therefore, it was of our interest to investigate the effect of arginylation on CRT dimerization/oligomerization.

In the present study, we demonstrate that arginylation increases CRT dimerization and oligomerization *in vitro*, mainly at low calcium concentrations, a similar condition to that required for *in vivo* CRT arginylation. In addition, arginylation does not induce global changes in the tertiary structure of CRT, but it confers a subtle destabilizing effect that could be related to an increase in a local structure fluctuation. Furthermore our results reveal that even when arginylated CRT (R-CRT) dimerization is not essential for its association to stress granules (SGs), R-CRT dimer formation through Cys146 is critical for the scaffolding of larger SGs which is crucial for the normal cellular recovery after heat shock in cultured cells.

2. Materials and methods

2.1. cDNA cloning, expression and purification of R-CRT-FLAG and CRT-FLAG proteins

The expression of the CRT-FLAG and R-CRT-FLAG recombinant proteins as poly-histidine (His_6)-tagged ubiquitin (Ub) fusions was performed in an *Escherichia* (*E.*) *coli* vector named Histidine-tagged Ubiquitin Expression (pHUE) and the fusion cleavage was performed by Usp2-cc, a His6-tagged deubiquitylating catalytic core (both plasmid vectors provided by Professor Rohan T. Baker; Molecular Genetics Group, The John Curtin School of Medical Research, The Australian National University) (Catanzariti et al., 2004). For the cloning of R-CRT-FLAG and CRT-FLAG cDNAs the coding sequence of mature hCRT (human CRT without signal peptide) was amplified by PCR from pCMV-Sport6-hCRT (cDNA provided by Professor Hugo L. Monaco; Biocrystallography Laboratory, University of Verona, Verona, Italy). The forward primer used in the amplification reaction of CRT-FLAG cDNA contains a Sac II restriction site (underlined), two codons that codify for two glycine residues (in bold) which are essential for cleavage by deubiquitylating enzymes, and the hCRT sequence (in italics) (5′-ATCCGCCGC**GGTGGA***GAGCCTGCCGTCTACTTCAAGG*-3′). For the amplification reaction of R-CRT-FLAG cDNA the forward primer further contains a codon that codifies to an arginine residue (lowercase) (5′-ATCCGCCGC**GGTGGA**cgt*GAGCCTGCCGTCTACTTCAAGG*-3′). The reverse primer is the same for both amplification reactions and contains a Kpn I restriction site (underlined), a FLAG-tagged sequence (in bold) and the hCRT sequence (in italics) (5′-ATCGGGGTACCCTA**GTCGTCGTCGTCTTTGTAGTC***CAGCTCGTCCTTGG-CCTGG*-3′). The PCR products were digested with the restriction enzymes Sac II and Kpn I and were cloned into the pHUE expression vector digested with the same endonucleases; the constructs were confirmed by DNA sequencing.

The His_6-Ub-CRT-FLAG and His_6-Ub-R-CRT-FLAG fusion proteins were expressed and purified from crude *E. coli* extracts by nickel-affinity chromatography under native conditions. Then these fusion proteins were cleavaged with Usp2-cc deubiquitylating enzyme to obtain CRT-FLAG and R-CRT-FLAG proteins. Briefly, overnight cultures of *E. coli* strain BL21(DE3) transformed with pHUE-CRT-FLAG, pHUE-R-CRT-FLAG and pHUsp2-cc were subcultured 1:10 into 500 mL Luria broth containing 50 μg/mL ampicillin and grown at 37 °C up to a late exponential phase (optical density: 0.6–0.8). Proteins expression was induced by adding isopropyl-1-thio-β-D-galactopyranoside (IPTG) to a final concentration of 0.4 mM for 4 h. An aliquot of each culture was collected for SDS-PAGE analysis of protein induction (Supplementary Figure 1, line 1). Cells collected by centrifugation were resuspended in 20 mL of buffer 2A [50 mM Na_2HPO_4/NaH_2PO_4 at pH 7.4, 300 mM NaCl, 20 mM imidazole, 20 mM β-mercaptoethanol [β-ME], 30% glycerol and 1 mM phenylmethylsulphonyl fluoride [PMSF]) and then they were frozen at −70 °C. The His_6-tagged proteins were purified in-batch by nickel-affinity chromatography under native conditions. The cells were thawed and then 15 mg of lysozyme were added, incubated on ice for 12 min and cells were lysed by sonication (3 times × 1 min bursts at 0 °C). The soluble protein fraction recovered by centrifugation at 4 °C (15 min at 15,000 × *g*). To the supernatants were added 1.5 mL of a 50% slurry of nickel-nitrilotriacetic acid (Ni-NTA) agarose beads in buffer 2A and then were placed on a rotary wheel at 4 °C for 1 h. The lysate/Ni-NTA mixtures were centrifuged 5 min at 550 × *g* and the supernatants were collected for SDS-PAGE analysis of unbound proteins (Supplementary Figure 1, line 2). The remaining Ni-NTA agarose pellets that contain the bound proteins were washed 4–6 times in 50 mL buffer 2A. The His_6-tagged proteins were eluted from the Ni-NTA resin in 2 fractions of 1 mL each with buffer 2A containing 500 mM imidazole (Supplementary Figure 1, lines 3–4). Both fractions were dialyzed overnight at 4 °C using buffer 50 mM Na_2HPO_4/NaH_2PO_4 at pH 7.4, 300 mM NaCl, 2 mM β-ME, 10% glycerol, 1 mM PMSF (Supplementary Figure 1, lines 6–7). Purified fusion proteins His_6-Ub-CRT-FLAG and His_6-Ub-R-CRT-FLAG were cleaved with Usp2-cc (1:10 ratio) 2 h at 37 °C and finally were incubated with 50 μL of Ni-NTA agarose beads and then were placed on a rotary wheel at 4 °C for 30 min to allow beads binding. The cleaved proteins were recovered in the supernatant fraction after centrifugation of the protein/Ni-NTA solutions (1–2 min at 1000 × *g*) (Supplementary Figure 1, lines 8–9). The protein concentration of each sample was determined by a Bradford assay (Pierce).

Supplementary material related to this article found, in the online version, at http://dx.doi.org/10.1016/j.biocel.2013.03.017.

2.2. Site-specific mutagenesis of hCRT (C146A-hCRT-ECFP)

The construct of the C146A-hCRT-ECFP mutant was generated using the method of site-specific mutagenesis by overlap extension. This method (Higuchi et al., 1988; Ho et al., 1989)

required two mutagenic primers, two flanking oligonucleotides, and three PCR to construct the C146A mutation (mutant numbering corresponds to the amino acid sequence of mature CRT). One pair of primers was used to amplify the DNA that contains the mutation site together with downstream sequences. The reverse primer (RM) contains the mutation (underlined and in bold) to be introduced into the wild-type template cDNA of hCRT [5′-GTAAACTCATCATCCTT**GGC**ACGGATGTCCTTGTTGATC-3′] whereas the forward primer (F2) contains a hCRT wild-type sequence composed of an EcoRI restriction site (underlined) and Kozak sequence (in bold) [5′-CTTCGAATTC**CCCGCCGCCACCATGC**TGC-3′]. The second pair of primers was used to amplify the DNA that contains the mutation site together with upstream sequences. The forward primer (FM) of this pair contains the mutation to be introduced into the template DNA and is complementary to primer RM [5′-GATCAACAAGGACATCCGT**GCC**AAGGATGATGAGTTTAC-3′], whereas the reverse primer (R2) contains a hCRT wild-type sequence and has a Kpn I restriction site (underlined) in its 5′ region [5′-CGGGGTACCCCCAGCTCGTCCTTGGCCTGGCC-3′]. The two sets of primers were used in two separate amplification reactions to amplify overlapping DNA fragments. The mutation of interest is located in the region of overlap and therefore in both sets of resulting amplified fragments. The overlapping fragments were mixed and, in a third PCR, amplified into a full-length hCRT DNA using primers F2 and R2 that bind to the 3′ and 5′ extremes respectively of the two initial fragments. The PCR product was digested with EcoRI and KpnI endonucleases and cloned into the pECFP-N1 (EYFP, enhanced yellow fluorescent protein) expression vector (Clontech Laboratories), and the construct was confirmed by DNA sequencing.

2.3. Dimerization-oligomerization assay

To induce dimerization and oligomerization of CRT-FLAG and R-CRT-FLAG, proteins were incubated in oligomerization buffer: 20 mM Tris, 10 mM Na_2HPO_4/NaH_2PO_4 (pH 7.4), 30 mM NaCl and 3% glycerol at different temperatures (37 °C–57 °C) for 30 min in the absence or in the presence of EDTA. Furthermore, R-CRT-FLAG was incubated at 37 °C for 30 min in the absence and presence of varying concentrations of EDTA (5–20 mM) and $CaCl_2$ (0.1–1 mM). After each treatment sample buffer (0.2 M Tris/HCl, pH 8.8,10% glycerol, 0.005% bromophenol blue) was added and samples were immediately subjected to native-PAGE to determine the degree of oligomerization.

2.4. Native-PAGE

The gels were prepared similarly to the technique described for SDS-PAGE (Laemmli, 1970), without SDS. The samples for these assays were prepared in a buffer containing 0.2 mM Tris/HCl, pH 8.8 10% glycerol and 0.005% bromophenol blue, without the addition of SDS and/or β-mercaptoethanol. The electrophoretic run was carried out at 100 V for 75 min in running buffer using a Tris/Glycine 25 mM/192 mM, pH 8.5. Furthermore, native gradient gels were prepared with a gradient maker system (Amersham Biosciences Gradient Maker) with 12% and 4% acrylamide solutions. After electrophoresis, gels were transferred to nitrocellulose membrane for subsequent immunodetection with anti-FLAG monoclonal antibody (Sigma) or with polyclonal anti-R-CRT by means of Western Blot (WB) technique described above.

2.5. Circular Dichroism

Near-UV-CD measurements were made with a Jasco J-810 spectropolarimeter using a 1-cm path length quartz cell. The temperature in the cell was controlled with a circulating water bath and the actual temperature in the sample was measured with a thermocouple inserted in the cell. For spectrum acquisition, protein concentration used was 0.4 mg/mL. Scan speed was set at 50 nm/min, with a 2-s response time, 0.2 nm data pitch, and 2-nm bandwidth. Measurements were carried out in the 250–320 nm region. Each spectrum was an average of six scans. The contribution of the buffer (oligomerization buffer) was subtracted in all spectra. Mean residue molar ellipticity was calculated according to $[\theta] = \theta$. MRW/lc where MRW is the mean residue molecular weight calculated from the protein sequence, θ is the measured ellipticity (in degrees) at a given wavelength, l is the cuvette path length in mm, and c is the protein concentration in g/mL. Thermal denaturation curves were obtained by monitoring the ellipticity at 280 nm. We set a continuous mode of acquisition, with a 1-s response time, 1-s data pitch, and 2-nm bandwidth. Protein concentration was 0.14 mg/mL, similar to those of protein oligomerization assays. The temperature setting in the bath was manually increased in steps of 1–2 °C, to obtain a constant increase in the sample temperature of 60 °C/h. Data acquired within temperature intervals of 1 °C were averaged. The fraction folded was calculated assuming a two state transition as: $f_f = (\theta - \theta_2)/(\theta_1 - \theta_2)$, where θ is the measured ellipticity at any temperature, θ_1 is the ellipticity of the folded protein (measured at 20 °C) and θ_2 is the ellipticity of the unfolded protein (measured at 65 °C). Thermal denaturation midpoint temperatures (Tm's) were determined by fitting the denaturation curve to a Boltzmann sigmoid equation using the Origin 7.0 software.

2.6. Cell cultures

All cell lines were grown as described previously (Carpio et al., 2010). CRT−/− and CRT+/+ mouse EF cell lines were a gift from Dr. M. Michalak (Department of Biochemistry, University of Alberta, Edmonton, Canada). To induce heat shock stress conditions, cells were incubated for 30 min at 42 °C. Cells were transfected with Lipofectamine LTX with Plus™ Reagent (invitrogen) following the manufacturer's protocol for plasmid DNA transfection.

2.7. Immunofluorescence

For immunofluorescence, the cells were grown on glass coverslips to 60% confluence. The procedure employed was similar to that already described (Decca et al., 2007). Briefly, after treatment, cells were washed with PBS, fixed with 4% PFA for 20 min, permeabilized with 0.1% Triton X-100 for 10 min, rinsed three times with PBS, and non-specific binding sites were blocked with 10% FBS in PBS for 60 min. Rabbit anti-R-CRT pAb (1:100) (custom made by Eurogentec, Seraing, Belgium), mouse anti-CRT mAb (1:1000) (BD Biosciences) and goat anti-(TIA-1) (T-cell intracytoplasmic antigen 1) pAb (1:100) (Santa Cruz Biotechnology) primary antibodies were added for 1 h. The secondary antibodies were the same as in Decca et al. (2007).

2.8. Image acquisition and analysis

Confocal cellular images were captured with an inverted Zeiss LSM 5 Pascal laser confocal microscope (Carl Zeiss) with the same technology already described (Carpio et al., 2010). Confocal images were captured with an Olympus FV1000 (Olympus, Japan) laser confocal microscope. Fluorescence intensity was quantified using ImageJ software. Both R-CRT and TIA-1 aggregates size ($pixels^2$) was determined from confocal images. Granules in each image file were defined using the threshold function in Image J (http://rsb.info.nih.gov.80/ij/). Granule areas were then calculated using the analyze particles feature. For calculations, all images were taken at 60× magnification and the entire image was quantified thereby ensuring a uniform pixel size. The data were then imported into Excel for subsequent analysis. For presentation, granule size

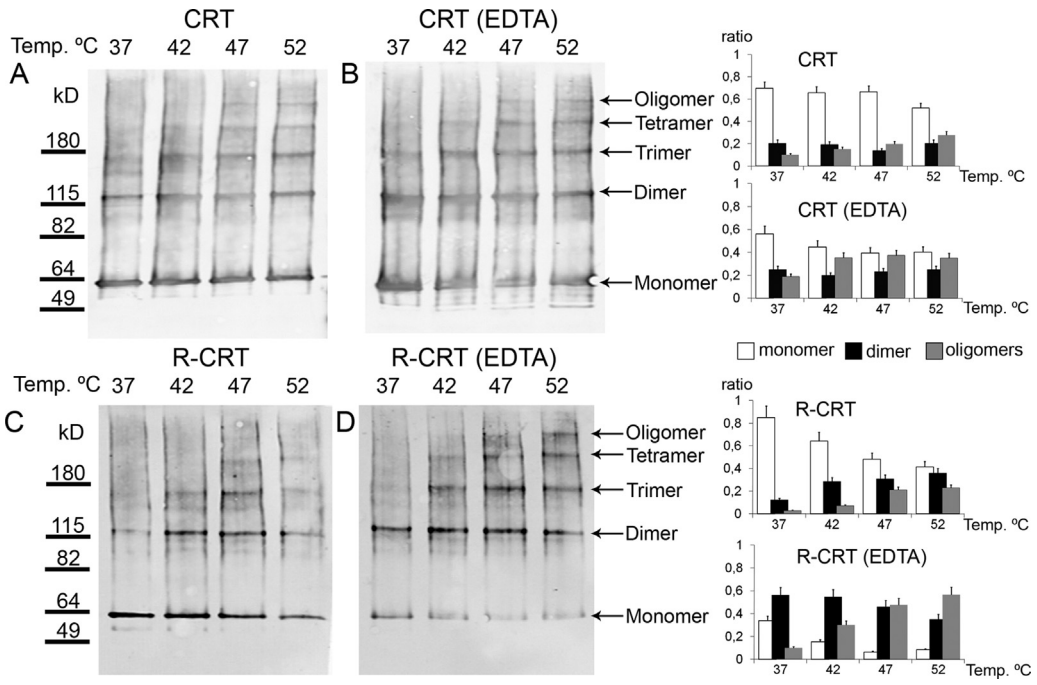

Fig. 1. Oligomerization of CRT and R-CRT as a function of temperature. Equivalent amounts of CRT (A and B) or R-CRT (C and D) were incubated at different temperatures (37, 42, 47, 52 °C) for 30 min in the absence (A and C) or presence (B and D) of EDTA. Then, the samples were subjected to electrophoresis in polyacrylamide gradient native gel (4–12%) and protein bands were visualized with anti-FLAG mAb by WB. The MW of the different bands was calculated using standard MW. The right panels correspond to the quantification of the protein bands, represented in white (monomer), black (dimer) and gray (oligomers: trimer, tetramer and higher oligomers). The values are the means ± SD of two independent experiments.

distributions were all normalized to 500 particles and the normalized distributions were compared using the *F*-test for two sample variance. We define as small aggregates: below 49 pixels^2; and large aggregates: above 64 pixels^2.

2.9. Assessment of apoptosis

Redistribution of plasma membrane phosphatidylserine (PS) was used as a marker of apoptosis and was assessed by annexin V Phycoerythrin (PE) (BD Biosciences) following the manufacturer's protocol. Briefly, after treatment, cells were washed and allowed to recover in fresh medium for 24 h. 1×10^6 cells per experimental conditions were collected, washed in phosphate-buffered saline (PBS), pelleted, and resuspended in incubation buffer (10 mM HEPES/NaOH pH 7.4, 140 mM NaCl, 2.5 mM $CaCl_2$) containing 1% annexin V and 1% 7-AAD or propidium iodide, to identify dead cells. Under these conditions, samples were kept in the dark for 15 min prior to analysis by flow cytometry on a FACSCantoII cytometer (BD Biosciences) using BD FACSDiva software.

3. Results

3.1. Arginylation promotes a high degree of CRT dimerization

To examine the effect of CRT arginylation on the dimerization and oligomerization process, equivalent amounts of CRT and R-CRT recombinant proteins were incubated at different temperatures (37, 42, 47 or 52 °C) for 30 min in the absence or in the presence of EDTA. Then, samples were subjected to electrophoresis on polyacrylamide gradient gels (4–12%) in non-denaturing conditions (Native-PAGE). CRT and R-CRT bands were visualized by WB using an anti-FLAG mAb which recognizes the C-terminal FLAG-tag of the recombinant proteins (see details in Section 2). The molecular weight (MW) of each band was calculated with native MW standards. The electrophoretic pattern for CRT under these conditions showed the complex equilibrium of CRT oligomerization (Fig. 1). We observed CRT as monomers, dimers, trimers, tetramers and even larger oligomers; for simplicity we will refer as "oligomers" to the sum of all the species from trimer to higher MW species (Fig. 1). Incubation of CRT at increasing temperatures leads to an increase in the amount of oligomers (mainly heavier oligomers) with the consequent decrease of the monomeric form (Fig. 1A); no significant modification on the dimer proportion was observed. These results are in agreement with those described for human placental CRT (Jorgensen et al., 2003).

To investigate the oligomerization process of CRT we performed the oligomerization assay in the presence of EDTA. At all temperatures tested, the amount of oligomers (Fig. 1B) was higher than in the non-EDTA incubation condition, whereas the dimer proportion only slightly increased (Fig. 1A and B). The depletion of Ca^{2+} resulted in a shift to lower temperatures for the oligomerization process; thus the relative amounts of monomers, dimers and oligomers at 42 °C in the presence of EDTA are comparable to those at 52 °C in the non-EDTA incubation conditions. It has been previously reported that Ca^{2+}depletion promotes CRT destabilization (Li et al., 2001), and enhances its polypeptide binding, chaperone activity and oligomerization (Rizvi et al., 2004).

On the other hand, the oligomerization assay for R-CRT showed a very different scenario. In the absence of EDTA, we observed a significant increases in R-CRT dimers and oligomers as the incubation temperature increased (Fig. 1C). Although the oligomerization of R-CRT was similar to that of non-arginylated CRT its dimerization was clearly enhanced. In the presence of EDTA, dimerization of R-CRT was further increased, being dimers the predominant specie at 37 °C (Fig. 1D, lane 1). It should be noticed that this experimental condition resembles the low Ca^{2+}environment of cell cytoplasm, suggesting that dimeric R-CRT could be the physiologically relevant form of this protein within the cytosol. In addition, incubation of R-CRT in the presence of EDTA at higher temperatures (47 and 52 °C) also increased protein oligomerization (Fig. 1D, lanes 2–4)

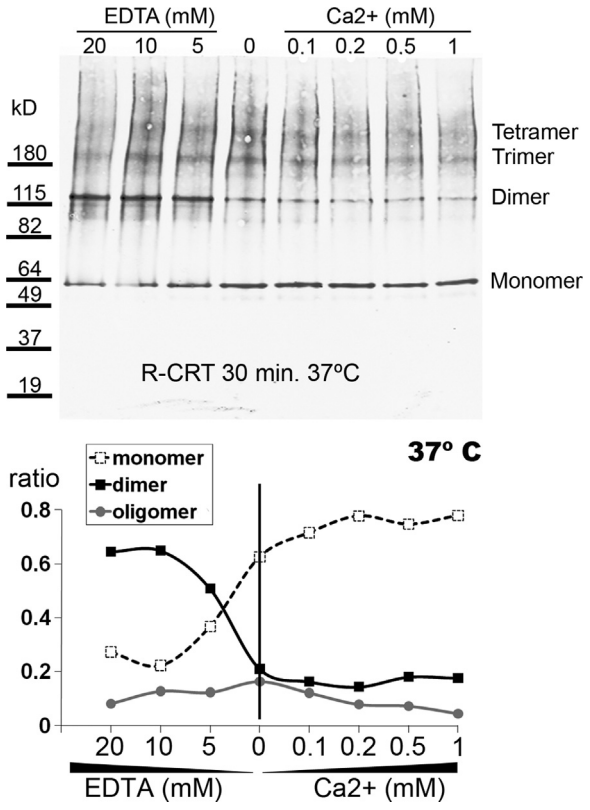

Fig. 2. Dimerization and oligomerization of R-CRT as a function of Ca^{2+} concentration. Equivalent amounts of R-CRT-FLAG were incubated at different concentrations of EDTA or Ca^{2+} at 37 °C for 30 min. Then, the samples were subjected to electrophoresis in polyacrylamide gradient native gel (4–12%) and protein bands were visualized with anti-R-CRT pAb by WB. At physiological temperatures (37 °C) the degree of aggregation of R-CRT varies between the monomer (white square) and the dimer (black square), being favored the dimer formation in the absence of Ca^{+2} (lanes 1–3) and the monomer in the presence of this ion (lanes 5–8). The MW of the different bands was calculated using a standard MW. The low panel corresponds to the quantification of the protein bands, represented in dashed line (monomer), black line (dimer) and gray line (oligomers).

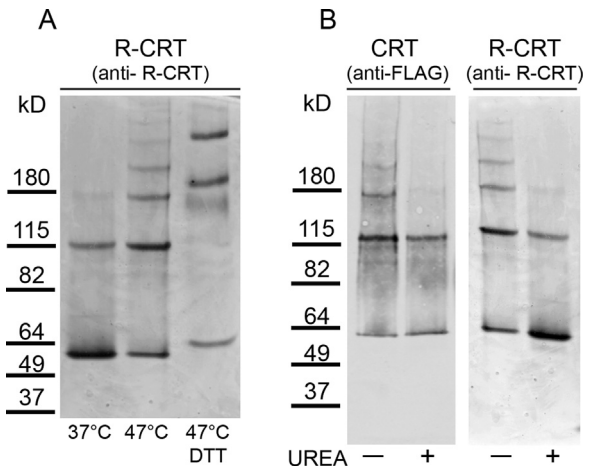

Fig. 3. Dimerization and oligomerization of CRT and R-CRT (A) R-CRT-FLAG heated for 30 min in the absence or presence of 5 mM DTT. Lane 1, R-CRT-FLAG incubated at 37 °C; lane 2, R-CRT-FLAG incubated at 47 °C, lane 3, R-CRT-FLAG incubated at 47 °C in the presence of 5 mM DTT. (B) CRT-FLAG and R-CRT-FLAG heated with or without the addition of urea to the sample before heating. Lane 1, CRT-FLAG incubated for 30 min at 47 °C without urea (control), lane 2, CRT-FLAG in 8 M urea followed by 30 min incubation at 47 °C; lane 3, R-CRT-FLAG incubated for 30 min at 47 °C without urea (control), lane 4, R-CRT-FLAG in 8 M urea followed by 30 min incubation at 47 °C.

being the proportion of R-CRT oligomers significantly higher than CRT oligomers under the same conditions (Fig. 1B, lanes 2–4). These results suggest that R-CRT is more susceptible than CRT to dimerize and oligomerize and that both processes are modulated by Ca^{2+}concentration.

Assuming that the formation of the disulfide-bridged dimer is a consequence of the exposure of the free SH-Cys146, our result point out that arginylation increases protein flexibility at least near the Cys146, enhancing the SH exposure, and therefore its dimerization. Additionally, arginylation *per se* does not promote higher oligomerization states since in the absence of EDTA the amount of CRT and R-CRT oligomers are similar (Fig. 1A and C). Only the combination of both arginylation and Ca^{2+}depletion enhances oligomerization.

To further study the R-CRT aggregation in relation to the Ca^{2+} concentration, equal amounts of R-CRT were incubated at different concentrations of EDTA or Ca^{2+} at 37 °C for 30 min (Fig. 2). The rise of EDTA concentration up to 20 mM induces a threefold increase in the R-CRT dimers at expense of the monomeric form (Fig. 2, lanes 1–3). On the other hand, an increase in Ca^{2+} up to 1 mM did not modify the dimer proportion and only a small reduction of the oligomer fraction was observed (Fig. 2, lanes 5–8). Clearly, the occupancy of the high affinity Ca^{2+}binding site precludes R-CRT dimerization, whereas the occupancy of the low affinity binding site does not significantly alter R-CRT self association. Our results show that at 37 °C, R-CRT oscillates mainly between the monomer and the dimer, in response to changes in Ca^{2+}concentrations. Under stress conditions, the R-CRT aggregation and association to SGs also involve changes in Ca^{2+} concentrations (Carpio et al., 2010); therefore, was deemed reasonable to consider if R-CRT dimerization affects the SGs assembly and its association in cells.

To elucidate the nature of the binding of R-CRT monomers to form dimers, we induced dimerization and oligomerization of R-CRT by incubating the protein at 47 °C in the presence of a reducing agent DTT to avoid disulfide bridges. Under these conditions, we did not detect dimer formation, but we observed that R-CRT renderer into larger oligomers, (Fig. 3A, lane 3), indicating that R-CRT dimers are mainly formed by the covalent disulfide bridge. Besides, after incubation under denaturing conditions (8 M urea), pre-formed oligomers but not dimers are reverted for both R-CRT and CRT proteins (Fig. 3B). These results, in agreement with the proposed mechanism for CRT oligomerization, show that R-CRT oligomerization is formed by non-covalent interactions and that R-CRT dimerization involves intermolecular disulfide bridges. However, we cannot rule out the existence of others non-disulfide-bridged dimers, since the proportion of dimers slightly decreased after urea treatment (Fig. 3B, lane 4) probably these non-covalent dimers were not seen upon DTT treatment (Fig. 3A, lane 3) because they are part of the oligomers.

3.2. Additional characterization of R-CRT by thermal denaturation

The above results are consistent with a mayor exposure of the free SH-Cys146 in R-CRT, which enhances disulfide-bridged R-CRT dimerization. To address if the overall structure of CRT become modified upon arginylation or if it promotes only a local conformational rearrangement, we performed near-UV circular dichroism (CD) of CRT and R-CRT. Near UV-CD spectrum arises from the asymmetric environment of aromatic residues and is a characteristic of protein tertiary structure, which can be assessed by this technique. CRT and R-CRT have the same near UV-CD spectrum at 26 °C (Fig. 4A), with overall characteristics similar to those previously published for CRT (Bouvier and Stafford, 2000): positive peaks around 270, 280 and 287 nm and a shoulder between 292 and 300 nm. The great amount of aromatic residues in these proteins results in overlapped bands and precludes particular residue assignment. The increase in temperature results

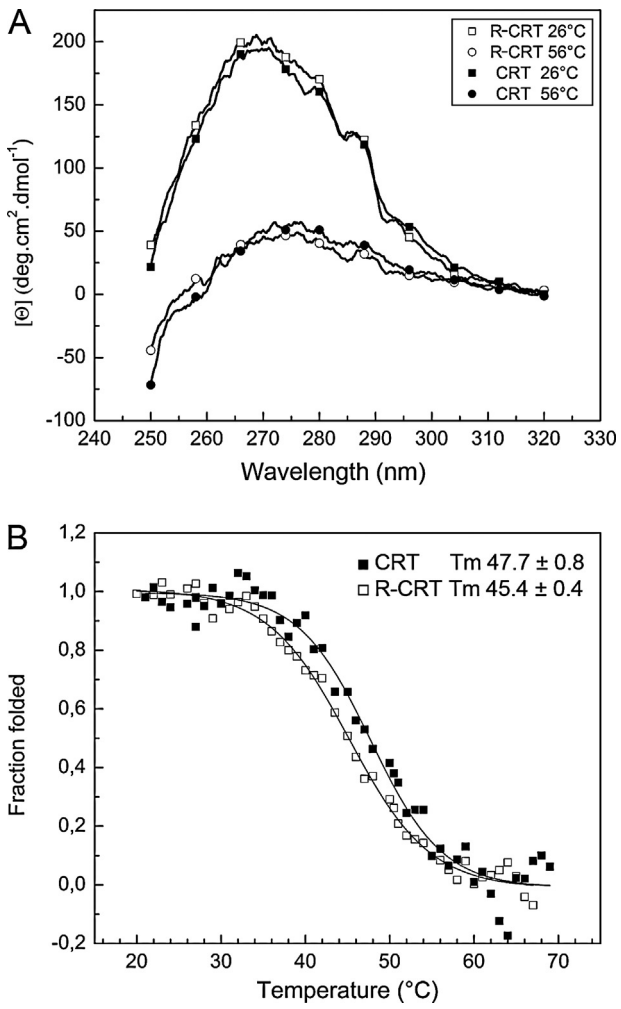

Fig. 4. Near-UV-CD spectra of CRT and R-CRT. (A) spectra of CRT at 26 °C (black square) and 56 °C (black circle) and of R-CRT at 26 °C (white square) and 56 °C (white circle) in oligomerization buffer with 5 mM EDTA. (B) Thermal denaturation curves of CRT (black square) and R-CRT (white square) monitored by ellipticity at 280 nm. The values of Tm are the means ± SD from three independent experiments with $p = 0.013$.

in a decrease of near-UV ellipticity for both R-CRT and CRT as seen in the spectra at 56 °C, due to the loss of protein tertiary structure upon thermal unfolding. Spectra showed in Fig. 4A were taken in the presence of 5 mM EDTA, condition in which the major differences between CRT and R-CRT were expected according to the oligomerization assays. Spectra in the absence of EDTA (not shown) were essentially indistinguishable from that showed in Fig. 4A. Thermal denaturation curves monitored by ellipticity at 280 nm showed a cooperative transition centered at 47.7 °C for CRT and at 45.4 °C for R-CRT (Fig. 4B). Thus, arginylation reduced CRT thermostability in about 2 °C.

Our results indicate that arginylation does not induce global changes in the tertiary structure of CRT, but it confers a subtle destabilizing effect. A similar decrease in thermostability was found by mutations of some hydrophobic residues within the CRT globular domain. These mutated proteins also presented an increased chaperone activity probably due to enhanced exposure of hydrophobic surfaces (Jeffery et al., 2011). In addition, enhanced chaperone activity also correlates with calreticulin oligomerization (Rizvi et al., 2004). We propose that arginylation increases local structure fluctuation and promotes a major exposure of hydrophobic surface, consistent with the R-CRT reduced thermostability and it major tendency to form dimers and oligomers.

3.3. Proteins dimerization is relevant for the scaffolding of larger SGs

Cells subjected to conditions such as heat shock, oxidative or ER stress display a Ca^{2+} homeostasis disturbance that induces a decrease in cytosolic Ca^{2+} levels, besides the aggregation and association of R-CRT to SGs (Carpio et al., 2010). Based on the *in vitro* results showed above, our next aim was to study the role of R-CRT dimerization on SGs formation and R-CRT association.

The first approach was to reduce and prevent disulfide bridge formation of cytoplasmic covalent protein dimers by exposing cells to DTT. As it has been previously demonstrated when DTT is used at concentrations up to 2 mM in cells, it markedly reduces the formation of disulfide bridges in the cytosol and does not affect the PTMs of protein or alter the normal secretory pathway (Lodish and Kong, 1993). We explored if this reducing agent affected PTMs involved in SGs formation, i.e. the phosphorylation of eIF2α, which is a required signal for the assembly of SGs in cells exposed to environmental stress (Anderson and Kedersha, 2008). For this, cells were incubated in the absence or in the presence of DTT and subjected or not to heat shock. Then, total proteins from cell lysates were subjected to SDS-PAGE and the phosphorylated (P) and total eif2α isoform proteins were analyzed by WB using eif2α-P and total eif2α antibodies, respectively. As shown in Fig. 6A, the levels of eif2α-P in cells treated with DTT is comparable to control cells, showing that DTT does not induce eIF2α phosphorylation. However, the levels of eif2α-P in cells subjected to heat shock increase as compared to the levels detected in control cells, which is an indication of stress induction. Moreover, cells exposed to heat shock in the presence or absence of DTT display similar eif2α-P levels. These results reveal that DTT does not alter posttranslational phosphorylation under control or stress conditions. Note that the expression of total eif2α does not vary at the different conditions tested (Fig. 6A).

Since DTT did not affect PMT involved in SGs formation, we studied if dimerization impaired by DTT treatment had an effect on SGs formation and R-CRT association to them. We performed immunofluorescence assays in cells incubated without or with 2 mM DTT, or subjected to heat shock (20 min 42 °C) or to a combination of both treatments. Anti-R-CRT pAb, anti-CRT mAb and anti-TIA-1 pAb were used for the immunodetection of R-CRT, CRT and SGs, respectively. Untreated Cos-7 cells showed the typical scarce cytoplasmic-like immunostaining for R-CRT (Fig. 5A, b), a reticular localization for CRT (Fig. 5A, a) and a nuclear/cytoplasmic localization for TIA-1 (Fig. 6B, a), which is a protein that continuously shuttles between the nucleus and the cytoplasm (Kedersha et al., 2000). When cells were exposed to DTT for 20 min the distribution of R-CRT and CRT was not altered (Fig. 5A, d–f). Under these conditions, SGs formation was not observed (Fig. 5A, d–f) which correlated with the low levels of eIF2α-P (Fig. 6A). When the cells were subjected to heat shock, R-CRT content increased and displayed a cytoplasmic aggregation (Fig. 5A, h), which colocalized with the SGs marker TIA-1 (Fig. 6B, g–i). A granulometric digital analysis of these R-CRT aggregates (Fig. 5B and C) revealed that under heat shock treatment, the number of larger aggregates increased, whereas the small R-CRT aggregates were decreased (Fig. 5C, green bars) in comparison to the untreated (Fig. 5B, blue bars) or the DTT treated cells (Fig. 5B, red bars). These results indicate that a pool of small R-CRT aggregates increases and gradually gather (upon heat shock) to form larger R-CRT aggregates which colocalize with larger SGs (Fig. 6B, g–I). On the other hand, when cells were subjected to heat shock in the presence of DTT, the number and size of R-CRT aggregates (Fig. 5C, purple bars) were similar to those determined in untreated cells (Fig. 5B, blue bars). Under these experimental conditions the size of the SGs were smaller than the ones observed under

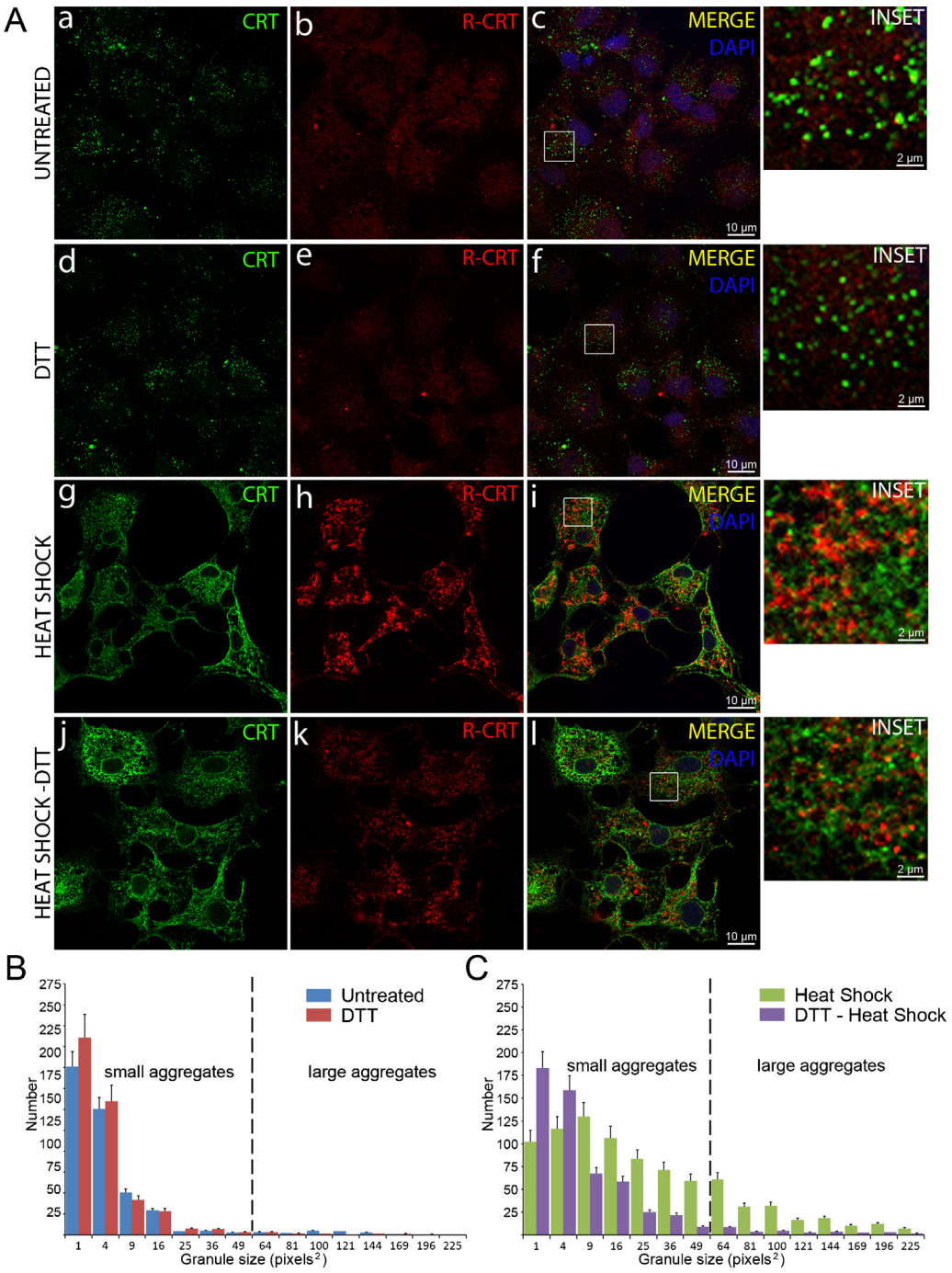

Fig. 5. Protein dimerization is involved in the scaffolding of larger R-CRT aggregates. (A) Cos-7 cells untreated (a–c) or treated with DTT (2 mM for 20 min) (d–f), heat shock (42 °C, 30 min) (g–i) or with DTT-heat shock (j–l) were analyzed by immunofluorescence using anti-R-CRT pAb and anti-CRT mAb. By confocal microscopy R-CRT does not colocalize with CRT after any of the treatments (A; c, f, i and l). (B and C) The confocal images acquired were subjected to a granulometric analysis and shown in a size distribution graph. Values are means ± SD from at least 60 cells analyzed in three independent experiments.

heat shock; however the association of small R-CRT aggregates with small SGs was not impaired (Fig. 6B, l).

These results indicate that in Cos-7 cells the DTT treatment does not alter neither the SGs formation nor the association of R-CRT to them induced by heat shock, however the scaffolding of larger SGs was impaired by the presence of DTT, suggesting that disulfide-bridges of SGs components (presumably R-CRT dimerization) are involved in scaffolding of larger SGs.

We also explored the implication of the scaffolding of larger SGs under the stress response and its impact on cellular survival. For this, cells were incubated in the absence or in the presence of DTT, and subjected or not to heat shock. Then, the cells were washed and allowed to recover in fresh medium for 24 h, time at which apoptosis was determined by flow cytometry with annexin-V staining. As shown, untreated cells as well as DTT treated cells (Fig. 7a and b) displayed lower levels of apoptosis (<=20%) as compared to heat shock treated cells (Fig. 7c), which partially recovered from stress and having up to 30% of apoptotic cells. However, cells under heat shock-DTT, in which formation of larger SGs is impaired, have less capacity to recover from stress, showing that 45% of the cells were in apoptosis (Fig. 7d). These results together with the above described, suggest that protein dimerization is important for

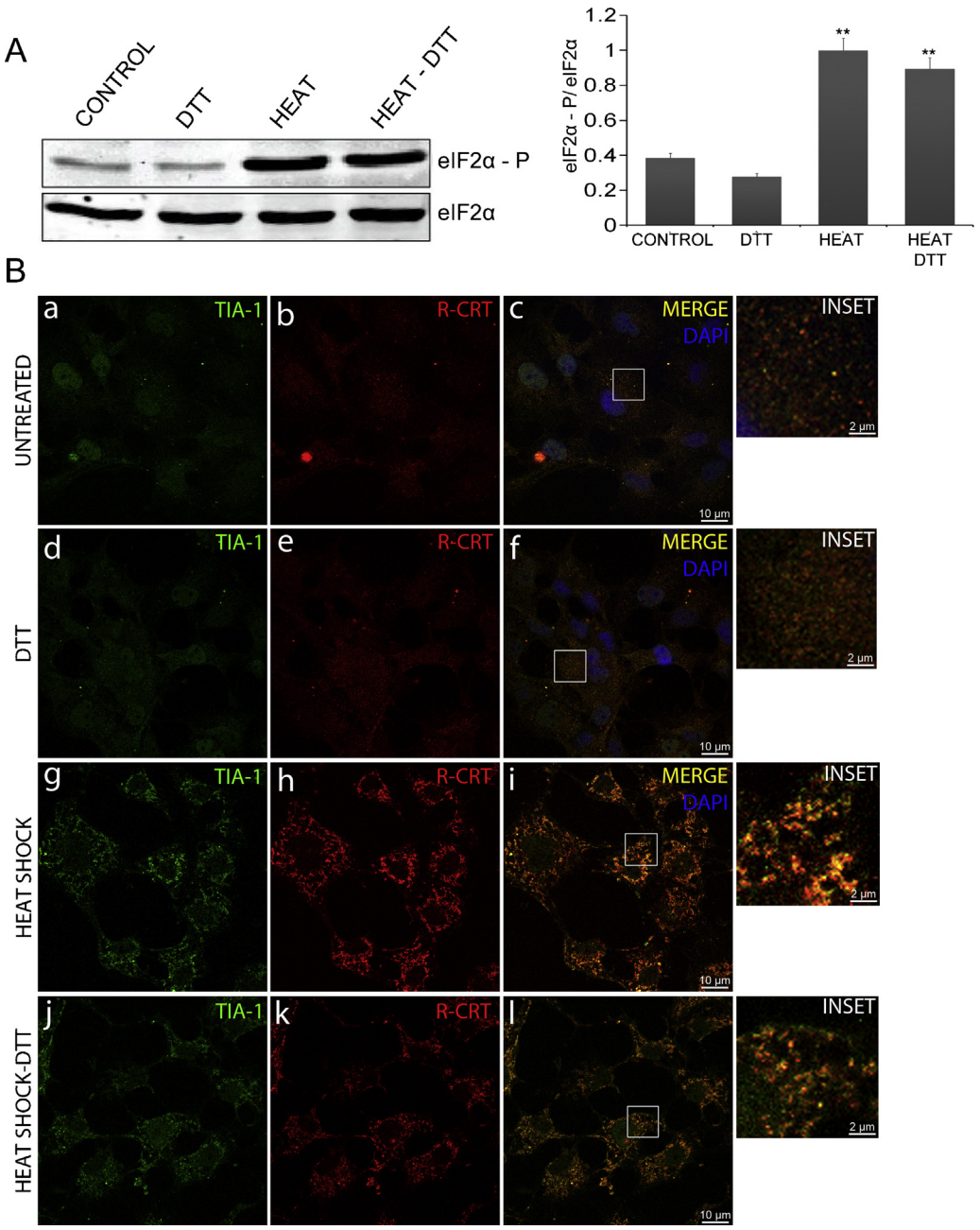

Fig. 6. Protein dimerization is involved in the scaffolding of larger SGs. (A) Cos-7 cells were incubated in the presence or absence of DTT heated at 42 °C or not for 20 min. Then, cells were lysed with RIPA and the samples were subjected to WB analysis against eif2α and eif2α-P antibodies. The bands intensity was quantified using ImageJ programme and the eif2α-P/eif2α ratio was calculated. Statistical significance was calculated with ANOVA. **, $p < 0.002$ indicate significant changes between the levels of eif2α-P proteins in cells subjected to heat shock with or without DTT with respect to those expressed in non heated cells. (B) Cos-7 cells untreated (a–c) or treated with DTT (2 mM, 20 min) (d–f), heat shock (40 °C, 30 min) (g–i) or with DTT-heat shock (j–l) were analyzed by immunofluorescence using anti-R-CRT pAb and the anti-TIA-1 mAb. Yellow pseudo-color in the merged images and in the enlarged regions of interest (insets) represents co-localization of R-CRT and TIA-1 as seen by confocal microscopy in heat shock conditions (i) and heat shock- DTT (l). Values are means ± SD from at least 60 cells analyzed in two independent experiments.

normal cellular recovery after heat induced stress and that R-CRT may be implicated in this process by inducing scaffolding of larger SGs.

3.4. The R-CRT dimerization is necessary for the scaffolding of larger SGs

We have previously shown that the arginylation of CRT is necessary for the association of CRT to SGs nevertheless SGs are formed in the absence of CRT or ATE1 enzyme (CRT−/− and ATE1−/− cells), suggesting that neither CRT nor arginylation are necessary for the formation of these complexes (Carpio et al., 2010). To study how R-CRT influences the assembly of SGs, CRT+/+ and CRT−/− cells were subjected to heat shock and the formation of SGs was analyzed by immunofluorescence using anti-TIA-1 pAb antibody. We observed that in both cell lines, heat shock induces SGs assembly (Fig. 8A, b and d). However, the SGs size distribution was different between both cell lines, as determined by a granulometric digital analysis. In CRT+/+ cells subjected to heat shock, the number of SGs (Fig. 8B, black bars) increases as compared to untreated cells (Fig. 8B, gray bars). These results imply that in heat shock treatment, the

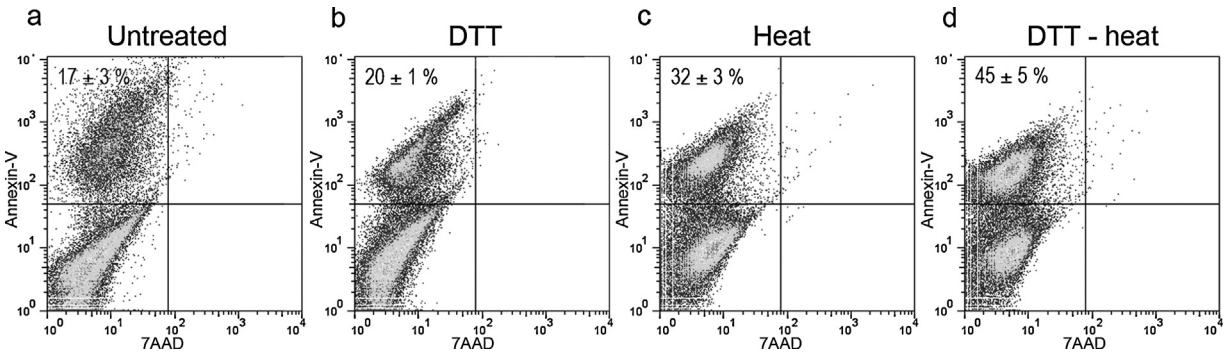

Fig. 7. Protein dimerization is necessary for normal recovery after heat-shock induced stress. CRT+/+ cells incubated in the absence (a) or in the presence of DTT 2 mM (b), subjected to heat-shock for 30 min (c) or to a combination of heat in the presence of DTT (d) were allowed to recover from stress for 24 h. Then, apoptosis was determined by annexin-V and 7-Aminoactinomycin D (7-AAD) staining of the cells. Representative flow cytometry dot blots of each condition are shown. Data are means ± SD from three independent experiments. 100% values correspond to 50,000 cells.

total amount of SGs (smaller and larger) increases. In CRT−/− cells subjected to heat shock (Fig. 8A, d) the larger SGs assembly was impaired (Fig. 8C, black bars) as compared to CRT+/+ cells (Fig. 8B, black bars). Moreover, the number of small SGs in CRT−/− cells under heat shock (Fig. 8C, black bars) was increased when compared to that determined in CRT−/− untreated cells (Fig. 8C, gray bars). Taking into account that these cells lack CRT and hence there is no cytoplasmic R-CRT which is the only isoform that associates to SGs, and the experiments done with DTT (Figs. 5 and 6), suggest that R-CRT is an important player for SGs

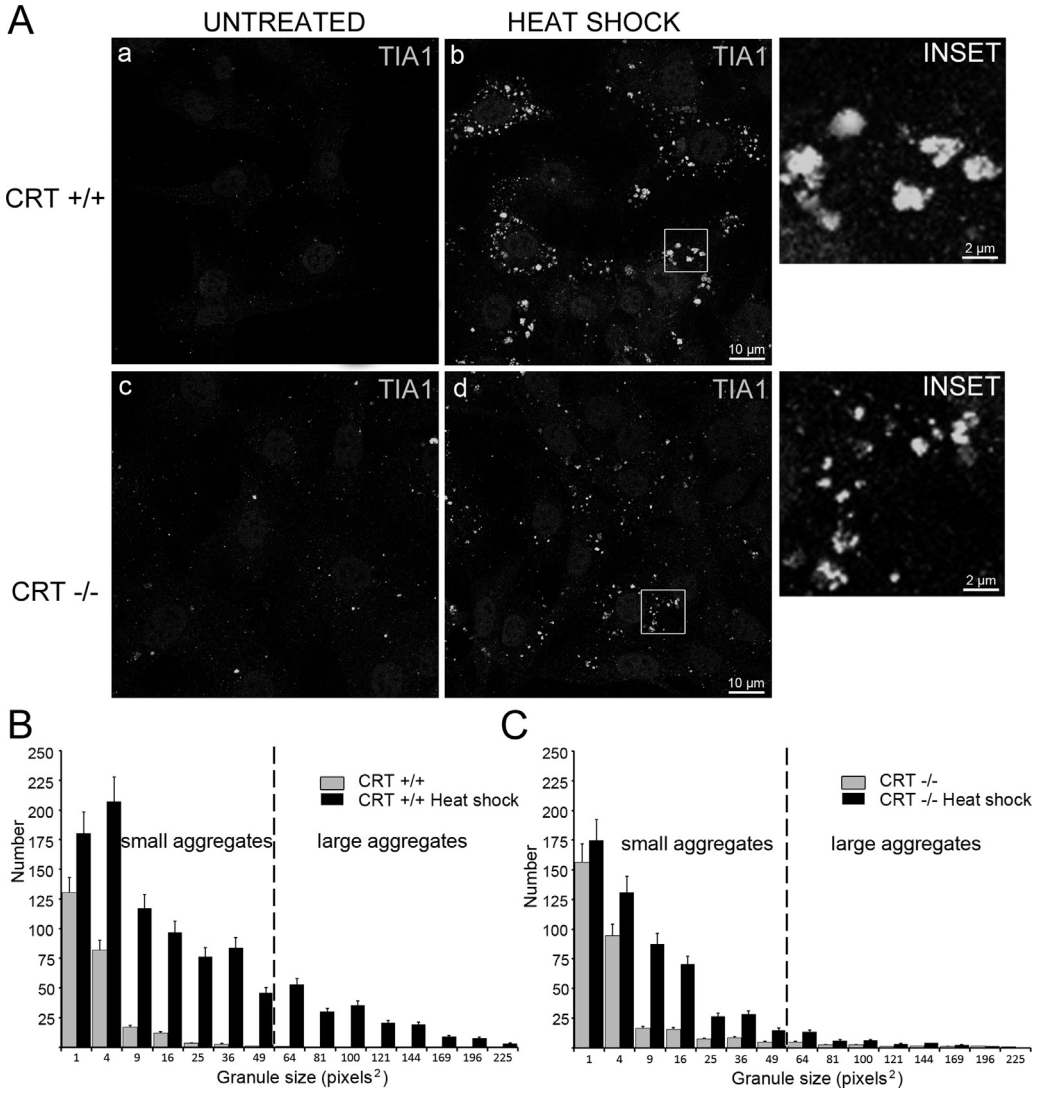

Fig. 8. R-CRT is involved in the scaffolding of larger SGs. Control CRT+/+ and CRT−/− cells (A, a and c) or exposed to heat shock (42 °C, 30 min) (A, b and d) were analyzed by immunofluorescence using an anti-TIA1 mAb. The confocal images acquired were subjected to a granulometric analysis and shown in a size distribution graph (B and C). Values are means ± SD from at least 60 cells analyzed in two independent experiments.

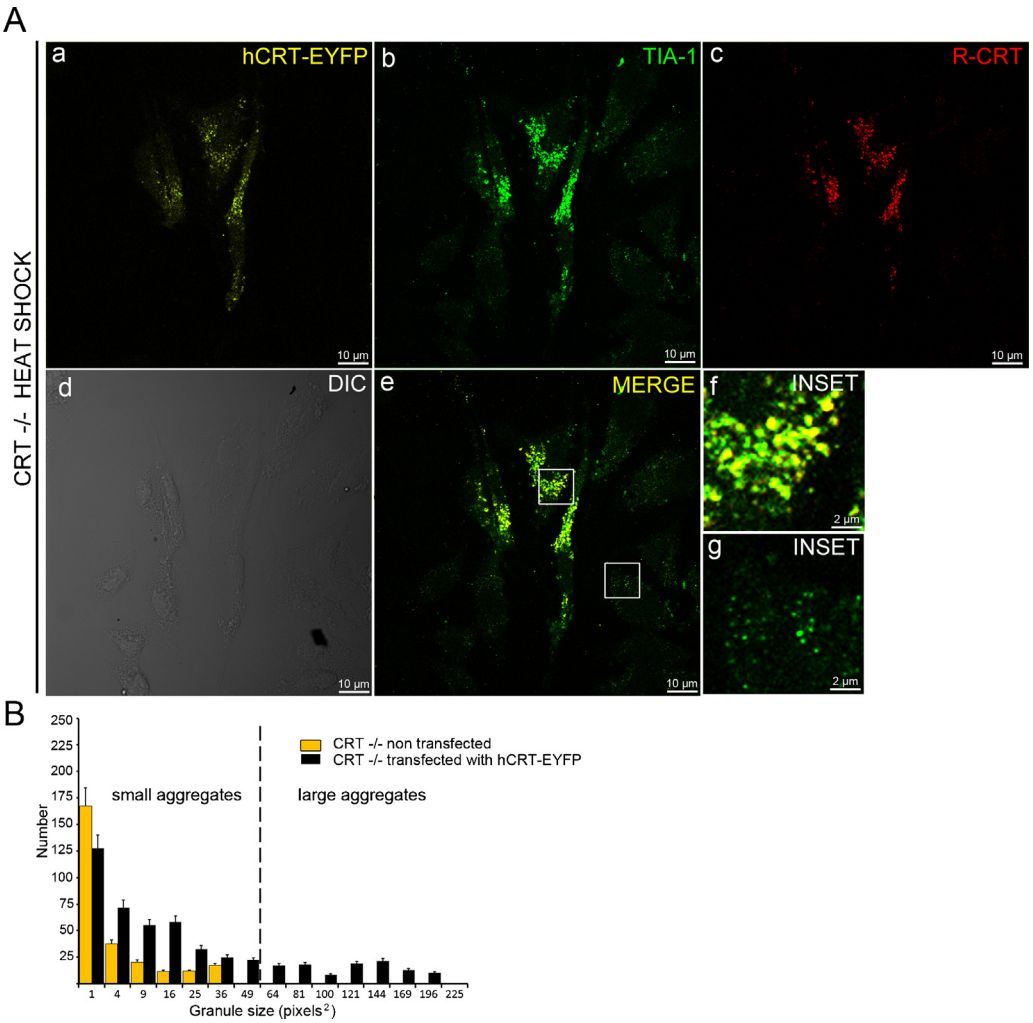

Fig. 9. R-CRT rescue the scaffolding of larger SGs in CRT−/− cells. (A) CRT−/− cells transfected with hCRT-EYFP exposed to heat shock (42 °C, 30 min) were analyzed by immunofluorescence using an anti-R-CRT pAb (A, c) and anti-TIA1 mAb (A, b). Yellow pseudo-color in the merged image (A, e) and the enlarged regions of interest (insets) represents co-localization of R-CRT and TIA-1 in hCRT-EYFP transfected cells (A, f) and TIA-1 in non-transfected cells (A, g). (B) The confocal images acquired were subjected to a granulometric analysis and shown in a size distribution graph. Values are means ± SD from at least 60 cells analyzed in two independent experiments.

assembly, involved in the recruitment of small SGs and/or in the scaffolding of larger SGs under heat shock.

To reinforce the findings described above and establish the role of R-CRT dimer in the scaffolding of SGs, immunofluorescence assays were performed in CRT−/− cells transiently transfected with hCRT–EYFP and then subjected to heat shock stress. As described by Carpio et al. (2010), transfected cells express CRT in the ER (Fig. 9A, a) with a concomitant appearance of cytoplasmic R-CRT (Fig. 9A, c). Interestingly, in these cells an increased in the number of larger SGs was observed (Fig. 9A, b) and measurement by granulometric analysis (Fig. 9B, blacks bars) as compared to CRT−/− non-transfected cells (Fig. 9A, b and B, yellow bars). The larger SGs colocalized with R-CRT in the CRT−/− transfected cells (Fig. 9A, e and f). This finding demonstrated that the presence of cytoplasmic R-CRT, which is the only CRT isoform that has the ability to associate to SGs, is able to rescue the impaired scaffolding of larger SGs observed in non-transfected CRT−/− cells under heat shock conditions (Fig. 8A, d and Fig. 9A, g).

3.5. R-CRT dimerization through Cys146 is involved in the scaffolding of larger SGs

To demonstrate that dimerization of R-CRT is involved in the scaffolding of the larger SGs a construct of CRT was developed where Cys146 was mutated to alanine and fused to a cyan fluorescence protein (C146A-hCRT-ECFP). CRT−/− cells were transiently transfected with this construct and then subjected to heat shock stress to induce the SGs formation. These transfected cells show a similar number and size of SGs than the non transfected cells (Fig. 10A, e–g and B). Thus, the ability to form larger SGs in CRT−/− cells transfected with the CRT mutated in Cys146 was not rescued (Fig. 10A, f and B, blacks bars) as occurred in CRT−/− cells transfected with CRT-EYFP under the same conditions (Fig. 9A, e–f and B, black bars).

Although the scaffolding of larger SGs was not rescued, the association of R-CRT to SGs was not altered in the CRT−/− transfected cells with C146A-CRT (Fig. 10A, e and f). Besides, in these cells, CRT was expressed in the ER (Fig. 10A, a) with a concomitant appearance of cytoplasmic R-CRT (Fig. 10A, c), as compared to non-transfected cells. However, a quantification of cytoplasmic R-CRT (Fig. 10C) showed that R-CRT levels in CRT−/− cells transfected with C146A-hCRT-ECFP (Fig. 10A, c) are lower than those detected in hCRT-EYFP transfected cells (Fig. 9A, c). This observation suggests that Cys146 could be involved in the retrotranslocation of CRT from the ER or is important for the stability of both CRT outside of ER and/or R-CRT after its post-translational modification. In conclusion, these results demonstrate that the dimerization of R-CRT through Cys146 is not essential for its association to SGs but that it

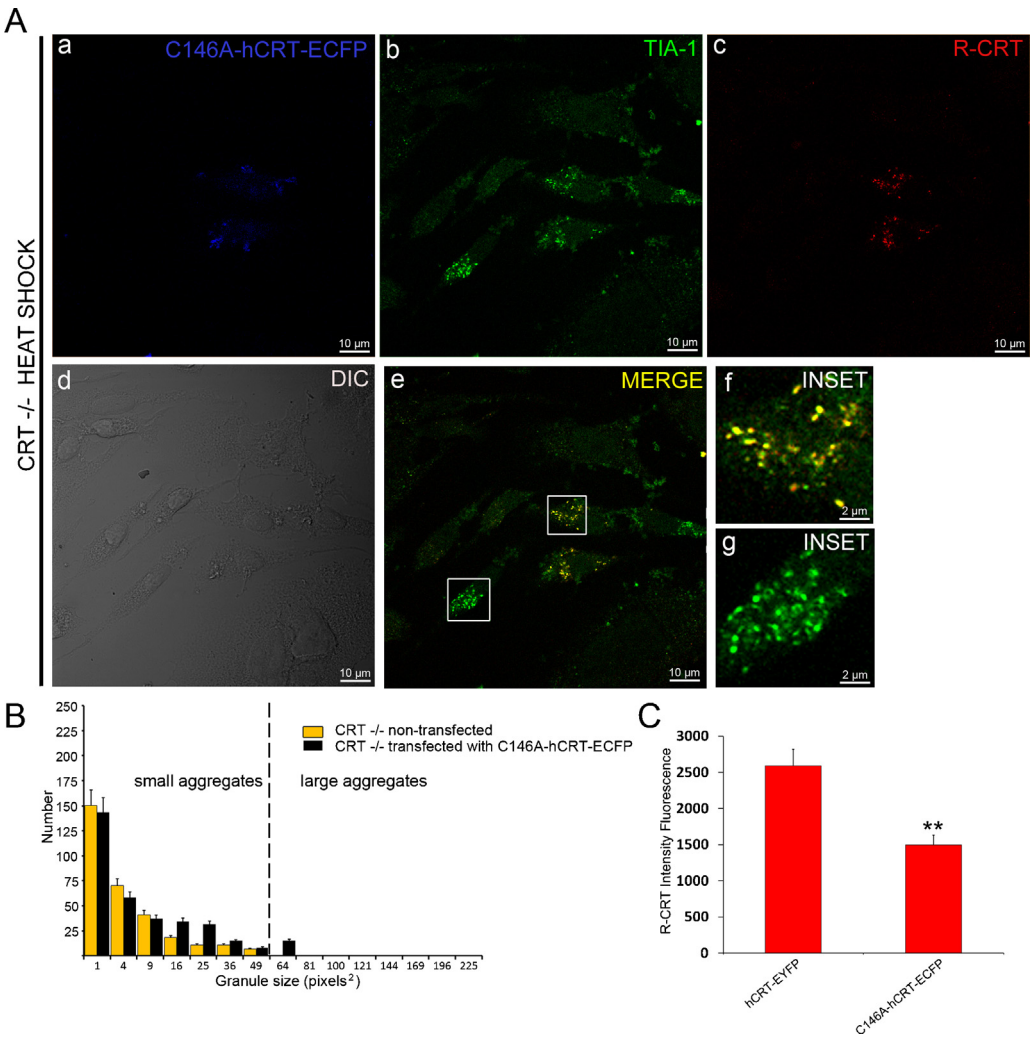

Fig. 10. R-CRT dimerization through Cys 146 is necessary for scaffolding of larger SGs. (A) CRT−/− cells transfected with C146A-hCRT-ECFP exposed to heat shock (42 °C, 30 min) were analyzed by immunofluorescence using an anti-R-CRT pAb (A, c) and anti-TIA1 mAb (A, b). Yellow pseudo-color in the merged image (A, e) and the enlarged regions of interest (insets) represents co-localization of R-CRT and TIA-1 in C146A-hCRT-ECFP transfected cells (A, f) and TIA-1 in non-transfected cells (A, g). (B) The confocal images acquired were subjected to a granulometric analysis and shown in a size distribution graph. Values are means ± SD from at least 60 cells analyzed in two independent experiments. (C) The amount of R-CRT in hCRT-EYFP and C146A-hCRT-ECFP transfected cells was quantified and expressed as fluorescence intensity per area as the mean ± S.D. of at least 60 cells analyzed. Statistical significance was calculated with ANOVA. **, $p < 0.002$ indicate significant changes.

is indeed involved in the scaffolding of larger SGs under heat shock stress.

4. Discussion

PTMs play a key role in several physiological events increasing the diversity of the proteome by the covalent addition of functional groups to proteins, proteolytic cleavage of regulatory subunits or degradation of proteins (Saha and Kashina, 2011). Among such modifications, an important role belongs to protein arginylation that is a global physiological regulator that modifies many proteins (Kwon et al., 2002; Kurosaka et al., 2012; Lee et al., 2012; Saha et al., 2012). In some cases arginylation is directly implicated in the arrangement of proteins as occurs with the non-muscle beta actin and actin related cytoskeleton proteins (Karakozova et al., 2006; Wong et al., 2007; Saha et al., 2010).

In this paper, we demonstrate that arginylation of CRT increases its tendency to form disulfide-bridged dimers, enhanced by Ca^{2+} depletion at physiological temperature. The relationship between arginylation and the exposure of free SH-Cys146 is not straightforward, since both residues are not close in the three-dimensional structure of the protein. The interaction, however, could occur in an intermolecular way. The resolution of the three-dimensional human CRT structure indicates that an arginine in the arginylation site can mediate intermolecular contacts within the other structural subunit (Chouquet et al., 2011). Thus, this residue could directly establish a primary non-covalent interaction between N-terminal arginine and a peptide binding domain of another CRT molecule, which would stabilize the formation of the disulfide bridge.

It has been previously demonstrated that Ca^{2+} depletion and heat shock induced CRT chaperone activity and correlates with an increase in CRT oligomerization, events that are related to the exposure of polypeptide binding sites of this protein (Rizvi et al., 2004; Jeffery et al., 2011). Here we demonstrated that arginylation provides another way that expand CRT interactions as it promotes a greater degree of dimerization when the protein is incubated at temperatures above 37 °C (Fig. 1), suggesting that arginylation induces a higher exposure of free SH-Cys146. Nevertheless, in conditions where arginylation and Ca^{2+} depletion are present, a synergic effect is observed with greater levels of CRT self-association. Dimerization prevails at 37 and 42 °C and oligomerization at higher temperatures. Interestingly, R-CRT at low Ca^{2+} concentration (EDTA) and 42 °C is the *in vitro* condition that mimics

heat shock stress that induces R-CRT association to SGs in cells (Fig. 6) (Carpio et al., 2010).

Extensive research has identified key components of SGs, their molecular interactions, and impact on reprogramming protein expression and cell survival. However, studies defining the signaling pathways that modulate SG assembly are recent, where many PTMs play key roles in their assembly and remodeling (Parker et al., 1996; Kedersha et al., 1999; Dolzhanskaya et al., 2006; Anderson and Kedersha, 2008; Xie and Denman, 2011). In this work, we demonstrate that an overall decrease in protein dimerization by a reducing agent impairs the scaffolding of larger SGs during the stress response. In a similar way, we found that CRT−/− cells are unable to form larger SGs as compared to CRT+/+ cells under the same conditions. As these CRT−/− cells do not express CRT or its arginine-modified isoespecie, R-CRT (which associates to SGs), this implies that R-CRT is involved in the clustering of larger SGs. Moreover, the scaffolding of larger SGs was rescued when CRT−/− cells were transfected with CRT-EYFP. However, when CRT−/− cells were transfected with a CRT that is mutated in the Cys146 the scaffolding of larger SGs was not rescued. These findings demonstrate that the presence of the R-CRT dimers through SH-Cys146 is essential for the scaffolding of SGs. Although larger SGs were not observed in CRT−/− cells transfected with C146A-CRT-ECFP, R-CRT was associated to small SGs indicating that while CRT arginylation is essential for its association to SGs its dimerization is not. Further studies will identify which other factors or PTMs could be implicated in CRT dimer formation.

It is known that the composition and morphology of SGs varies in different cells and upon the application of different stressors. However, a number of components are consistent across all types of stress (Guil et al., 2006; Buchan et al., 2011). Once the SG is formed by obligatory components, additional proteins are recruited to these structures, which alter the size, subcellular localization and affect the composition of SGs. (Wilczynska et al., 2005; Kedersha et al., 2005; Suzuki et al., 2009; Anderson and Kedersha, 2009; Bosco et al., 2010). Therefore, one hypothesis is that R-CRT is acting as a chaperone of proteins assisting the recruitment, folding or unfolding, and the assembly or disassembly of essential components within SGs where R-CRT is accumulated. The cell functional implication about scaffolding of larger SGs affected by R-CRT is still unknown. In this work, we found that cells subjected to heat shock-DTT, have a reduced ability to reverse the induced stress. Our hypothesis implies that the presence of R-CRT in SGs contributes to the recruitment of specific components, particularly in larger SGs, that will enhance the survival process of stressed cells. A recent work reveals that SGs formation might constitute a mechanism by which cancer cells resist bortezomib-mediated apoptosis (Fournier et al., 2010) and one key mechanism by which apoptosis is inhibited might involve up-regulation of the p21 mRNA in the SGs through CUGBP1 (Gareau et al., 2011) or CRT (Iakova et al., 2004). Therefore R-CRT could also act as an mRNA-binding protein capable of recruiting or stabilizing certain transcripts related to apoptosis into SGs.

The results shown in this work, together with our recent evidence related to R-CRT as a factor involved in stress induced apoptosis (Lopez Sambrooks et al., 2012) suggest that R-CRT has several roles in the cytoplasm, emerging as a novel protein implicated in the recognition, recruitment and/or stabilization of proteins or mRNA in SGs, further defining cell function and survival.

Acknowledgments

The authors are grateful to Drs. G. Pilar, B. Caputto and M.R. Galiano for their invaluable and helpful discussions, and G. Schachner, S. Deza, C. Mas, C. Sampedro, P. Abadie and P. Crespo for excellent technical assistance. This work was supported by grants from the Agencia Nacional de Promocion Científica y Technologica (BID 1728/OC-AR PICT No 1661), CONICET and SECyT Universidad Nacional de Córdoba. M.E.H, G.G.M, M.B.D. and E.S.D. are members of the Research Career of CONICET and M.A.C. and C.L.S are recipients of a fellowship from CONICET.

References

Afshar N, Black BE, Paschal BM. Retrotranslocation of the chaperone calreticulin from the endoplasmic reticulum lumen to the cytosol. Molecular and Cellular Biology 2005;25:8844–53.
Anderson P, Kedersha N. Stress granules: the tao of RNA triage. Trends in Biochemical Sciences 2008;33:141–50.
Anderson P, Kedersha N. RNA granules: post-transcriptional and epigenetic modulators of gene expression. Nature Reviews Molecular Cell Biology 2009;10:430–6.
Baksh S, Michalak M. Expression of calreticulin in *Escherichia coli* and identification of its Ca^{2+} binding domains. Journal of Biological Chemistry 1991;266:21458–65.
Barra HS, Rodriguez JA, Arce CA, Caputto R. A soluble preparation from rat brain that incorporates into its own proteins (14C)arginine by a ribonuclease-sensitive system and (14C)tyrosine by a ribonuclease-insensitive system. Journal of Neurochemistry 1973;20:97–108.
Bibi A, Agarwal NK, Dihazi GH, Eltoweissy M, Van Nguyen P, Mueller GA, Dihazi H. Calreticulin is crucial for calcium homeostasis mediated adaptation and survival of thick ascending limb of Henle's loop cells under osmotic stress. International Journal of Biochemistry and Cell Biology 2011;43:1187–97.
Bongiovanni G, Fissolo S, Barra HS, Hallak ME. Posttranslational arginylation of soluble rat brain proteins after whole body hyperthermia. Journal of Neuroscience Research 1999;56:85–92.
Bosco DA, Lemay N, Ko HK, Zhou H, Burke C, Kwiatkowski Jr TJ, et al. Mutant FUS proteins that cause amyotrophic lateral sclerosis incorporate into stress granules. Human Molecular Genetics 2010;19:4160–75.
Bouvier M, Stafford WF. Probing the three-dimensional structure of human calreticulin. Biochemistry 2000;39:14950–9.
Buchan JR, Yoon JH, Parker R. Stress-specific composition, assembly and kinetics of stress granules in *Saccharomyces cerevisiae*. Journal of Cell Science 2011;124:228–39.
Carpio MA, Lopez Sambrooks C, Durand ES, Hallak ME. The arginylation-dependent association of calreticulin with stress granules is regulated by calcium. Biochemical Journal 2010;429:63–72.
Catanzariti AM, Soboleva TA, Jans DA, Board PG, Baker RT. An efficient system for high-level expression and easy purification of authentic recombinant proteins. Protein Science 2004;13:1331–9.
Chouquet A, Païdassi H, Ling WL, Frachet P, Houen G, Arlaud GJ, Gaboriaud C. X-ray structure of the human calreticulin globular domain reveals a peptide-binding area and suggests a multi-molecular mechanism. PLoS One 2011;6:e17886, http://dx.doi.org/10.1371/journal.pone.0017886.
Corbett EF, Michalak KM, Oikawa K, Johnson S, Campbell ID, Eggleton P, et al. The conformation of calreticulin is influenced by the endoplasmic reticulum luminal environment. Journal of Biological Chemistry 2000;275:27177–85.
Decca MB, Carpio MA, Bosc C, Galiano MR, Job D, Andrieux A, et al. Post-translational arginylation of calreticulin: a new isospecies of calreticulin component of stress granules. Journal of Biological Chemistry 2007;282:8237–45.
Dolzhanskaya N, Merz G, Aletta JM, Denman RB. Methylation regulates the intracellular protein-protein and protein-RNA interactions of FMRP. Journal of Cell Science 2006;119:1933–46.
Farley AR, Link AJ. Identification and quantification of protein posttranslational modifications. Methods in Enzymology 2009;463:725–63.
Fournier MJ, Gareau C, Mazroui R. The chemotherapeutic agent bortezomib induces the formation of stress granules. Cancer Cell International 2010;10:12.
Gareau C, Fournier MJ, Filion C, Coudert L, Martel D, Labelle Y, et al. p21(WAF1/CIP1) upregulation through the stress granule-associated protein CUGBP1 confers resistance to bortezomib-mediated apoptosis. PLoS One 2011;6:e20254.
Gold LI, Eggleton P, Sweetwyne MT, Van Duyn LB, Greives MR, Naylor SM, et al. Calreticulin: non-endoplasmic reticulum functions in physiology and disease. FASEB Journal 2010;24:665–83.
Gonda DK, Bachmair A, Wunning I, Tobias JW, Lane WS, Varshavsky A. Universality and structure of the N-end rule. Journal of Biological Chemistry 1989;264:16700–12.
Guil S, Long JC, Caceres JF. hnRNP A1 relocalization to the stress granules reflects a role in the stress response. Molecular and Cellular Biology 2006;26:5744–58.
Higuchi R, Krummel B, Saiki RK. A general method of in vitro preparation and specific mutagenesis of DNA fragments: study of protein and DNA interactions. Nucleic Acids Research 1988;16:7351–67.
Ho SN, Hunt HD, Horton RM, Pullen JK, Pease LR. Site-directed mutagenesis by overlap extension using the polymerase chain reaction. Gene 1989;77:51–9.
Iakova P, Wang GL, Timchenko L, Michalak M, Pereira-Smith OM, Smith JR, et al. Competition of CUGBP1 and calreticulin for the regulation of p21 translation determines cell fate. EMBO Journal 2004;23:406–17.
Jeffery E, Peters LR, Raghavan M. The polypeptide binding conformation of calreticulin facilitates its cell-surface expression under conditions of endoplasmic reticulum stress. Journal of Biological Chemistry 2011;286:2402–15.

Jorgensen CS, Ryder LR, Steino A, Hojrup P, Hansen J, Beyer NH, et al. Dimerization and oligomerization of the chaperone calreticulin. European Journal of Biochemistry 2003;270:4140–8.
Kaji H, Novelli GD, Kaji A. A soluble amino acid-incorporating system from rat liver. Biochimica et Biophysica Acta 1963;76:474–7.
Karakozova M, Kozak M, Wong CC, Bailey AO, Yates 3rd JR, Mogilner A, et al. Arginylation of beta-actin regulates actin cytoskeleton and cell motility. Science 2006;313:192–6.
Kedersha N, Cho MR, Li W, Yacono PW, Chen S, Gilks N, et al. Dynamic shuttling of TIA-1 accompanies the recruitment of mRNA to mammalian stress granules. Journal of Cell Biology 2000;151:1257–68.
Kedersha N, Stoecklin G, Ayodele M, Yacono P, Lykke-Andersen J, Fritzler MJ, et al. Stress granules and processing bodies are dynamically linked sites of mRNP remodeling. Journal of Cell Biology 2005;169:871–84.
Kedersha NL, Gupta M, Li W, Miller I, Anderson P. RNA-binding proteins TIA-1 and TIAR link the phosphorylation of eIF-2 alpha to the assembly of mammalian stress granules. Journal of Cell Biology 1999;147:1431–42.
Khanna NC, Tokuda M, Waisman DM. Conformational changes induced by binding of divalent cations to calregulin. Journal of Biological Chemistry 1986;261:8883–7.
Kozlov G, Pocanschi CL, Rosenauer A, Bastos-Aristizabal S, Gorelik A, Williams DB, et al. Structural basis of carbohydrate recognition by calreticulin. Journal of Biological Chemistry 2010;285:38612–20.
Kurosaka S, Leu NA, Pavlov I, Han X, Ribeiro PA, Xu T, et al. Arginylation regulates myofibrils to maintain heart function and prevent dilated cardiomyopathy. Journal of Molecular and Cellular Cardiology 2012;53:333–41.
Kwon YT, Kashina AS, Davydov IV, Hu RG, An JY, Seo JW, et al. An essential role of N-terminal arginylation in cardiovascular development. Science 2002;297:96–9.
Labriola CA, Giraldo AM, Parodi AJ, Caramelo JJ. Functional cooperation between BiP and calreticulin in the folding maturation of a glycoprotein in *Trypanosoma cruzi*. Molecular and Biochemical Parasitology 2011;175:112–7.
Laemmli UK. Cleavage of structural proteins during the assembly of the head of bacteriophage T4. Nature 1970;227:680–5.
Lee MJ, Kim DE, Zakrzewska A, Yoo YD, Kim S, Kim ST, et al. Characterization of the arginylation branch of the N-end rule pathway in G-protein-mediated proliferation and signaling of cardiomyocytes. Journal of Biological Chemistry 2012;287:24043–52.
Li Z, Stafford WF, Bouvier M. The metal ion binding properties of calreticulin modulate its conformational flexibility and thermal stability. Biochemistry 2001;40:11193–201.
Lodish HF, Kong N. The secretory pathway is normal in dithiothreitol-treated cells, but disulfide-bonded proteins are reduced and reversibly retained in the endoplasmic reticulum. Journal of Biological Chemistry 1993;268:20598–605.
Lopez Sambrooks C, Carpio MA, Hallak ME. Arginylated calreticulin at the plasma membrane increases the susceptibility of cells to apoptosis. Journal of Biological Chemistry 2012;287:22043–54.
Mailhot G, Petit JL, Demers C, Gascon-Barre M. Influence of the in vivo calcium status on cellular calcium homeostasis and the level of the calcium-binding protein calreticulin in rat hepatocytes. Endocrinology 2000;141:891–900.
Michalak M, Groenendyk J, Szabo E, Gold LI, Opas M. Calreticulin, a multi-process calcium-buffering chaperone of the endoplasmic reticulum. Biochemical Journal 2009;417:651–66.
Paquet ME, Leach MR, Williams DB. In vitro and in vivo assays to assess the functions of calnexin and calreticulin in ER protein folding and quality control. Methods 2005;35:338–47.
Parker F, Maurier F, Delumeau I, Duchesne M, Faucher D, Debussche L, et al. A Ras-GTPase-activating protein SH3-domain-binding protein. Molecular and Cellular Biology 1996;16:2561–9.
Rai R, Wong CC, Xu T, Leu NA, Dong DW, Guo C, et al. Arginyltransferase regulates alpha cardiac actin function, myofibril formation and contractility during heart development. Development 2008;135:3881–9.
Rizvi SM, Mancino L, Thammavongsa V, Cantley RL, Raghavan M. A polypeptide binding conformation of calreticulin is induced by heat shock, calcium depletion, or by deletion of the C-terminal acidic region. Molecular Cell 2004;15:913–23.
Saha S, Kashina A. Posttranslational arginylation as a global biological regulator. Developmental Biology 2011;358:1–8.
Saha S, Mundia MM, Zhang F, Demers RW, Korobova F, Svitkina T, et al. Arginylation regulates intracellular actin polymer level by modulating actin properties and binding of capping and severing proteins. Molecular Biology of the Cell 2010;21:1350–61.
Saha S, Wang J, Buckley B, Wang Q, Lilly B, Chernov M, et al. Small molecule inhibitors of arginyltransferase regulate arginylation-dependent protein degradation, cell motility, and angiogenesis. Biochemical Pharmacology 2012;83:866–73.
Soffer RL. Enzymatic modification of proteins. 4. Arginylation of bovine thyroglobulin. Journal of Biological Chemistry 1971;246:1481–4.
Suzuki Y, Minami M, Suzuki M, Abe K, Zenno S, Tsujimoto M, et al. The Hsp90 inhibitor geldanamycin abrogates colocalization of eIF4E and eIF4E-transporter into stress granules and association of eIF4E with eIF4G. Journal of Biological Chemistry 2009;284:35597–604.
Wang WA, Groenendyk J, Michalak M. Calreticulin signaling in health and disease. The International Journal of Biochemistry & Cell Biology 2012;44:842-846.
Wijeyesakere SJ, Gafni AA, Raghavan M. Calreticulin is a thermostable protein with distinct structural responses to different divalent cation environments. Journal of Biological Chemistry 2011;286:8771–85.
Wilczynska A, Aigueperse C, Kress M, Dautry F, Weil D. The translational regulator CPEB1 provides a link between dcp1 bodies and stress granules. Journal of Cell Science 2005;118:981–92.
Wong CC, Xu T, Rai R, Bailey AO, Yates JR, Wolf 3rd YI, et al. Global analysis of posttranslational protein arginylation. PLoS Biology 2007;5:e258.
Xie W, Denman RB. Protein methylation and stress granules: posttranslational remodeler or innocent bystander? Molecular Biology International 2011;2011:137459.
Zhang JX, Braakman I, Matlack KE, Helenius A. Quality control in the secretory pathway: the role of calreticulin, calnexin and BiP in the retention of glycoproteins with C-terminal truncations. Molecular Biology of the Cell 1997;8:1943–54.